Integrated RF/Shim Coil Array for Parallel Reception and Localized B_0 Shimming in the Human Brain at 3T

Trong-Kha Truong[1], Dean Darnell[1], and Allen W Song[1]
[1]*Brain Imaging and Analysis Center, Duke University, Durham, NC, United States*

Introduction: Multi-coil shimming with a set of localized shim coils[1,2] can provide a more effective shimming of high-order susceptibility-induced B_0 inhomogeneities than conventional whole-body spherical harmonic shim coils. However, it requires an additional shim coil array outside[1] or inside[2] the RF coil array, which takes up valuable space in the magnet bore and increases the distance between the subject and the shim or RF coil array, respectively, resulting in a reduced shimming efficiency or SNR. In the latter case, a large gap is also required in the shim coil array to allow RF penetration and to reduce RF damping[2], which further compromises the shimming performance.

To address these limitations, we proposed a new concept termed integrated parallel reception, excitation, and shimming (iPRES)[3], which relies on a novel coil design that allows an RF current and a DC current to flow in the same coil simultaneously, thereby enabling parallel RF excitation/reception and B_0/B_1 shimming with a single coil array. Such an integrated RF/shim coil array can thus be placed close to the subject to maximize both the SNR and shimming performance.

The feasibility of this approach was demonstrated in proof-of-concept experiments performed in a phantom with a single loop[4] or a two-coil array[3] and simulations performed in the human brain with a 32- or 48-coil array[3,4]. Here, we further validate it in vivo by demonstrating its ability to perform parallel reception and localized B_0 shimming in the human brain at 3T, specifically to correct for susceptibility-induced geometric distortions in DTI.

Methods: Experiments were performed on a GE MR750 3T scanner with a GE 32-channel head coil array made of two rings of 11×6-cm coils. In this preliminary study, four adjacent coils around the prefrontal cortex were modified (**Fig. 1a**). A DC power supply and three inductors L_1 = 2700 nH were added to each coil to enable a DC current to flow in the closed loop, thereby generating an additional magnetic field that can be used for B_0 shimming (**Fig. 1b**). Each coil was connected to its DC power supply through a shielded twisted pair cable and two chokes L_2 = 680 nH to prevent electromagnetic interference and RF leaking. The Q factor of the coils remained the same.

In a one-time calibration step, five B_0 maps were acquired on a uniform phantom with a gradient-echo sequence (TR = 1 s, TE = 4.5 / 5.5 ms, voxel size = 2×2×2 mm). The first four were acquired with a DC current of 500 mA separately applied in each modified coil. The last one was acquired without DC current and subtracted from the other ones to remove background B_0 inhomogeneities, thus yielding four basis B_0 maps representing the B_0 field generated by each coil (**Fig. 2a**).

A B_0 map was then acquired on a healthy subject after 2nd-order shimming of the whole brain with the spherical harmonic shim coils of the scanner (**Fig. 2b**). The optimal DC currents to shim the prefrontal cortex were computed by minimizing the root-mean-square error between this B_0 map and a linear combination of the four basis B_0 maps in that brain region (computation time < 5 s).

DTI data were acquired without and with optimal DC currents using a twice-refocused spin-echo single-shot EPI sequence (TR = 5 s, TE = 79 ms, voxel size = 2×2×2 mm, b-factor = 800 s/mm^2, 25 diffusion directions). Undistorted images were also acquired with a fast spin-echo sequence for anatomical reference (TR = 3 s, TE = 85 ms, voxel size = 1×1×2 mm).

Results: Even after conventional spherical harmonic shimming, the DTI images remain affected by large susceptibility-induced distortions in the prefrontal cortex (**Fig. 3a,c**). Applying the DC currents in the integrated RF/shim coil array can reduce these distortions with no SNR penalty (**Fig. 3b,d**). The average/maximum DC currents were 388/500 mA. No significant coil heating was observed.

Discussion: In this initial study, the maximum DC current was limited to 500 mA, but this limit can easily be increased to improve the shimming performance by reducing the resistance of the coils. In addition, while this proof-of-concept study only used four coils to shim the prefrontal cortex, extension to 32 or more coils to shim the whole brain is straightforward and will further improve the shimming performance, particularly when combined with dynamic shimming (i.e., with DC currents updated in real time for the acquisition of each slice). Finally, while the proposed method was used to correct for distortions in EPI, it can also be applied to correct for other susceptibility artifacts, such as blurring in non-Cartesian imaging or signal loss in gradient-echo imaging (e.g., for fMRI).

Conclusion: The integrated RF/shim coil array can perform parallel reception and localized B_0 shimming in the human brain at 3T, while maximizing both the SNR and shimming performance as compared to conventional multi-coil shimming, which will be valuable for many applications.

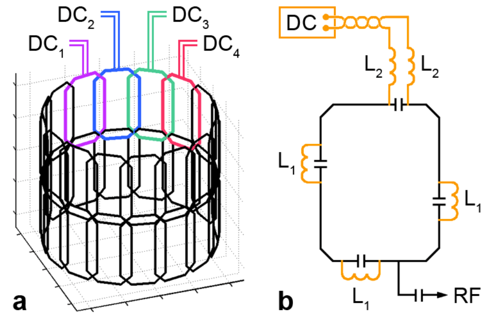

Fig. 1: Integrated RF/shim head coil array for parallel reception and localized B_0 shimming (**a**). Schematic circuit of one of the four modified coils, showing the DC power supply and the inductors added to generate a DC current in the loop (**b**).

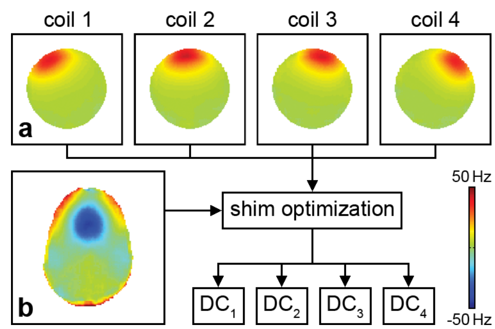

Fig. 2: Basis B_0 maps acquired on a phantom with a DC current of 500 mA separately applied in each modified coil (**a**). B_0 map acquired in vivo without DC current, showing large susceptibility-induced B_0 inhomogeneities in the prefrontal cortex (**b**).

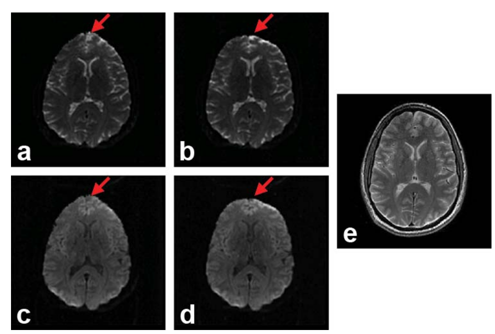

Fig. 3: Baseline (b = 0) (**a**,**b**) and mean diffusion-weighted (**c**,**d**) images acquired without (**a**,**c**) and with (**b**,**d**) DC currents. Anatomical image (**e**). The arrows show a reduction of susceptibility-induced distortions in the prefrontal cortex.

References: 1. Juchem C et al. MRM 2011;66:893–900. 2. Juchem C et al. JMR 2011;212:280–8. 3. Han H et al. MRM 2013;70:241–7. 4. Stockmann J et al. ISMRM 2013;21:665. This work was in part supported by NIH grants R01EB012586 and R01EB009483.